

Multiple-order moments of the transient electromagnetic response of a one-dimensional earth with finite conductance – theory

Terry J. Lee¹ and Richard S. Smith²

¹ GPO Box 1984, Canberra, ACT, 2601, Australia

² Harquail School of Earth Sciences, Laurentian University, 935 Ramsey Lake Rd, Sudbury, Ontario, P3E 2C6, Canada

Right running head: Multiple-order moments of a finite conductance

This is an accepted manuscript. The Version of Record of this manuscript has been published and is available in *Exploration Geophysics*,

Published 15 May 2020

DOI: <http://www.tandfonline.com/> <https://doi.org/10.1080/08123985.2020.1760715>.

Abstract. The concept of moments of the electromagnetic response is useful in electromagnetic interpretation. Analytic formulae exist for low-order moments of a few conductivity models, enabling source parameters such as time constant, depth, conductance and conductivity to be estimated from the measured moments of the electromagnetic response. However, most models for which analytic formulae exist have conductivity varying abruptly as a function of depth or position. In this paper, we have derived a procedure that allows moments of any order to be calculated for a conductivity which has finite conductance but can otherwise vary arbitrarily with depth. The horizontal loop transient electromagnetic step response is computed as a sum of residues. Integration of the step response over time yields a mathematical expression for a moment of any order. We illustrate the procedure for a Gaussian conductivity function which varies smoothly with depth. The Gaussian model produces results that agree in specific limits with the thin sheet, thick sheet and half-space cases.

Keywords: Electromagnetic methods, Interpretation, Layered, Conductivity, Airborne electromagnetics

Introduction

The moments of the time-domain electromagnetic impulse response is an integral transformation introduced by Smith and Lee (2002a; 2003). The n th-order impulse-response moment M^n is defined as

$$M^n = \int_0^{\infty} t^n \frac{\partial H(t)}{\partial t} dt, \quad (1)$$

where t is time and $H(t)$ is the step-response magnetic field. These moments are useful in the interpretation of electromagnetic data. Simple analytic formulae have been derived for the moments for the cases of a wire-loop conductor, a sphere (Smith and Lee, 2002a), a thin sheet, a thick sheet, a half-space (Smith and Lee, 2002b) and a small sphere in a uniform field (Smith and Lee, 2001). More complex formulae have been derived for more complex cases. For example, Desmarais (2019b) derived moment formulae for a sphere below an overburden using approximate closed form expressions for the time- and frequency-domain EM response (Desmarais, 2019a).

In general, in analytic formulae for low-order moments, the moment value is linearly related to parameters dependent on the conductivity, conductivity-thickness (conductance) and conductivity-radius-squared, so the moment formulae can be simply rearranged or inverted to estimate a conductivity parameter from a field-data moment. For example, when the top of the conductor is assumed to be at the ground surface, the conductance of a thin sheet or the conductivity of a half-space can be estimated from the first-order moment only (Smith et al., 2005). Another simple approach is to create a map of the first-order moment or resistive limit (Bournas et al., 2018). Moments have also been used for estimating the source parameters of a single sphere (Smith and Lee, 2001; Smith et al., 2003a). More sophisticated approaches involve using spherical models to generate discrete conductor sections (Smith and Salem, 2007), in analogy with conductivity depth sections (Macnae et al., 1991). The zeroth-order moments (or resistive limit) has also been used for modelling multiple spheres, as there is no interaction at the resistive limit and the moments can simply be summed (Hyde, 2002; Schaa and Fullagar, 2010, 2012; Fullagar and Schaa, 2014; Fullagar et al., 2015). The ratio of successively higher-order moments can be used to estimate the

time constant of a decay (Smith and Lee, 2002a; Guo et al., 2013). Most of the above examples relate to mineral exploration examples, but Snyder et al. (2010) and Hall (2014) have applied the moment concept to the interpretation of an unexploded ordnance (UXO) survey.

The mathematical transformation of the transient electromagnetic response to the moment domain assumes an ideal impulse or step response can be measured and integrated [e.g. using equation (1)].

However, no practical electromagnetic system has an ideal waveform and some are not even close to ideal. Smith and Lee (2002a) discuss the case when the impulse is smeared over a finite time and Smith (2000) and Smith and Wasylechko (2012) outline how to deal with a waveform that repeats and hence has a finite off-time. The precise way that the moments are calculated depends on the electromagnetic system used to measure the response. For the case of the GEOTEM system in a resistive area, see Smith and Lee (2020, paper submitted to *Exploration Geophysics*).

The works cited above have applied the moments to a variety of uses, from generating map images that can be interpreted, to providing a fast-forward solution that can be inverted to determine the depth, shape and properties of the material in the subsurface.

However, there are a limited number of moment solutions. Only zero- and first-order impulse response moments can be calculated for infinite conductance cases like the half-space (Smith and Lee, 2002b). Even for the thin and thick sheet, which both have a finite conductance, only zero-, first- and second-order impulse response moments can be calculated for the vertical-component moments and only the zeroth to third-order moments can be calculated for the radial-component moment (Smith and Lee, 2002b). The higher-order moments do not exist as they cannot be integrated mathematically, because the integrals are infinite. Each of the moments which do exist are sensitive to different depths (Smith and Lee, 2002b). Lee et al. (2003) derived a formula for the half-order impulse-response moment of a half-space and showed theoretically that this moment is sensitive to the material shallower than about 26 and 48 m, for the horizontal and vertical components, respectively when using the geometric configuration of the fixed-wing

GEOTEM/MEGATEM systems. The first-order moment is sensitive to material shallower than about 66 and 127 m for the same components and configuration.

Our motivation for the work of this paper is to broaden the class of models for which moment formulae can be derived and to be able to calculate the moments to higher order if required. Another of our long-term objectives is to use higher-order moments to resolve the conductivity at successively greater depth, but this is a topic of ongoing work and not reported here.

In the following, we analyze grounds with a conductance that is assumed finite but the conductivity has an arbitrary depth dependence. The assumption of finite conductance allows us to derive formulae for high-order moments. This involves evaluating the inverse Fourier transform as a sum of residues. Cases with infinite conductance are worthy of further analysis, but are beyond the scope of this paper. The mathematical derivations essentially are drawn from Gel'fans, and Levitan (1955), Titchmarch (1958) and Weidelt (1972). A variety of functional forms for the conductivity-depth profile have been treated in the literature. For example, Gray (1933) looked at a case where the conductivity decreases exponentially with depth; and Lee and Iqnetik (1994) have analyzed a case where the variation in conductivity can be represented by a simple growing or decaying exponential, $\sigma(z) = ae^{\pm bz}$. As an example of our general procedure, we have derived formulae for the moments when the conductivity has a Gaussian depth dependence, with the conductivity having a peak value at a specific depth and decreasing exponentially above and below. Our Gaussian distribution is thus more flexible than models considered previously. The numerical results we obtain for limiting cases of the Gaussian model are consistent with results already published for thin-sheet, thick sheet and half-space models.

The theory in this paper can assist interpretation of real data. For example, when the conductivity-depth function has a single peak, then we can use the moment formulae for a Gaussian distribution, to convert moments calculated from field data to three parameters: the depth at which the conductivity peaks, the conductivity at the peak and the narrowness of the Gaussian function. Images of these three quantities for

a survey area show features, potentially of exploration interest, that are not evident in standard images of the data (Smith and Lee, 2020, companion paper submitted to *Exploration Geophysics*).

Table 1: List of symbols

Symbol	Description	Equation where first defined
a	Transmitter loop radius	Before (2)
A_0	Peak conductivity as a function of depth	(21)
A	Secondary electric field amplitude, to be determined	After (4)
b	Narrowness parameter in Gaussian depth dependence of conductivity	(21)
B	Total electric field amplitude, to be determined	After (5)
c	Depth of peak Gaussian conductivity	(21)
C	Consistency factor	(22)
$E_1(r, z, t)$	Primary electric field	Before (4)
$E_2(r, z, t)$	Secondary electric field	Before (4)
$E_i(r, z, t)$	The i th component of the electric field, $i = r, \varphi, z$	Before (2)
$f(z, s, \lambda)$	Functional form for electric field accounting for an exponential depth dependence	(9)
$f_n(z, \lambda)$	Coefficient for series expansion of $f(z, s)$ in powers of s	(E4)
f', f'', f^*	Superscripts denotes the first and second derivatives w.r.t. z and complex conjugate of f (and f_n) respectively.	Before (D1)
F	Arbitrary function	Before (4)
$g(s, z)$	Arbitrary function of (s, z)	Before (A10)
h	Height of the transmitter above the surface $z = 0$	Before (2)
$H_i(r, z, t)$	Magnetic field in the i th coordinate direction	(2) and (3)
i	Subscript index	After (3)
$I(t)$	Transmitter current	After (3)
I_0	Peak current prior to switch off	After (3)
$I(z, c, \lambda)$	Integral function with arguments z, c and λ	(F1)
j	Subscript index	(13)
$J_l(x)$	Bessel function of l th order argument x	After (4) and (13)
$k_0^2 = \omega^2 \mu_0 \epsilon_0$	Wavenumber, in the upper half-space	After (4)
$k_1^2 = \mu \sigma i \omega + \mu \epsilon \omega^2$	Wavenumber, in the lower half-space	After (5)
$K(\omega, \lambda, z)$	Kernel function	(10)
$m_0 = \sqrt{\lambda^2 - k_0^2}$		(4)
M_i^n	The n th moment of the i th component of the step response	(17)
M_i^n	The n th moment of the i th component of the impulse response	(1)

q	Variable of integration for s	(B2)
r	Radial coordinate in cylindrical coordinate system	Before (2)
$R_E(\lambda)$	Residue of kernel of inverse Fourier transform	(14), (A21) and (B5)
s	Laplace transform variable $s = i\omega$	After (11)
S	Conductance	Before (2)
t	time	
$u(t)$	Heavyside step-on function	After (3)
z	Depth coordinate in cylindrical coordinate system	Before (2)
$\beta_n(\lambda)$	Coefficient for series expansion of kernel of inverse Fourier integral	(E2)
$\delta(\cdot)$	Dirac delta function, a function of x or t	After (3)
ε	Dielectric permittivity, subscript 0 denotes the free space value	After (4)
λ	Hankel transform variable	Before (4)
λ_i	The value of the Laplace transform variable at the i th pole of the kernel of the inverse Fourier transform.	(14) and (B3)
μ	Magnetic permeability in the ground, assumed to be uniform, subscript 0 denotes the free space value	(2) and (3)
π	3.1415926...	After (3)
$\sigma(z)$	Conductivity as a function of depth (z)	Before (2)
σ_i	Apparent conductivity or conductance from for thin-sheet or half-space cases respectively derived from the radial component when $i = r$ or the vertical component when $i = z$.	(22)
φ	Azimuthal coordinate in cylindrical coordinate system	Before (2)
$\phi(z, s, \lambda)$	Function describing the depth dependence of the electric field	After (5)
ϕ_s	Derivative w.r.t. s of $\phi(z)$	(A2)
ω	Angular frequency	(3)
*	A superscript * denotes complex conjugate	Before (D1)
' ''	The prime and double prime denotes a first and second derivative w.r.t. z	(7) and (A1)

Theory for general finite conductance case

We treat the case when the depth-integrated conductivity or conductance, $S = \int_0^{\infty} \sigma(z) dz$, is finite, where

$\sigma(z)$ is the variation of conductivity with depth, z . All symbols used in this paper are defined in Table 1.

We consider a horizontal loop transmitter, radius a , at a height h above a half-space. If we use a cylindrical (r, φ, z) coordinate system, then the electric field is purely azimuthal (Morrison et al. 1969), so $E = E_\varphi$.

Hence, Faraday's law reduces to the following two equations (Morrison et al., 1969).

$$-i\omega\mu H_r(r, z, \omega) = \frac{\partial E_\phi(r, z, \omega)}{\partial z}, \quad (2)$$

$$i\omega\mu H_z(r, z, \omega) = \frac{1}{r} \frac{\partial(rE_\phi(r, z, \omega))}{\partial r}, \quad (3)$$

where $H_i(r, z, \omega)$ is the magnetic field in the i th direction, ω is the Fourier transform variable or angular frequency, μ is the magnetic permeability and unlike Morrison et al. (1969) we assume a $e^{+i\omega t}$ time dependence. The transmitter current density is $J_s(r, z, t) = I(t)\delta(r - a)\delta(z + h)$, where $\delta(x)$ is the Dirac delta function. We assume a Heavyside step-on function for the current, $I(t) = I_0 u(t)$. We have chosen z to be increasing downward with depth. The interface is at $z = 0$ and the transmitter is at $z = -h$.

In the following we denote a Fourier transform pair by $E(t) \leftrightarrow E(\omega)$, where t is time and we adopt a negative exponential and a 2π normalization for the inverse transform. Following Morrison et al. (1969) we denote the Hankel transform pair of a function F by $F(r) \leftrightarrow F(\lambda)$, where λ is the Hankel transform variable. Because the only electric field is in the azimuthal direction, we can drop the subscript from the electric field. The electric field can be written as the sum of two terms, a primary E_1 and a secondary E_2 . Morrison et al. (1969) found that

$$E_1(r, z, \omega, \lambda) = \frac{\frac{1}{2}i\omega\mu_0 a I(\omega) J_1(\lambda a) e^{-m_0|h+z|}}{m_0}, \quad (4)$$

where $m_0 = \sqrt{\lambda^2 - k_0^2}$, $k_0^2 = \omega^2 \mu_0 \epsilon_0$, ϵ is the dielectric permittivity, J_1 is the Bessel function of order 1. and the subscripts zero represent the free-space values.

In the air, the solution is of the form $E_2(r, z, \omega, \lambda) = A e^{m_0 z}$, where A is yet to be determined. In the ground the total electric field satisfies (Morrison et al., 1969)

$$\frac{\partial^2 E}{\partial z^2} - (\lambda^2 - k_1^2)E = 0, \quad (5)$$

where $k_1^2 = \mu\sigma i\omega + \mu\epsilon\omega^2$. In the quasi static limit, henceforth assumed, $k_1^2 = \mu\sigma i\omega$ and $m_0 = \lambda$.

The total electric field below the ground can be written as $E = B\phi(z, \omega, \lambda)$, where B is a constant and ϕ is a solution of equation (5).

The boundary conditions at $z = 0$ are i) that the electric field is continuous, whence

$$E_1(0) + A = B\phi(0), \quad (6)$$

and ii) that the radial component of the magnetic field is continuous. From equation (2), this means that the vertical derivative of the electric field is continuous

$$-\lambda E_1(0) + \lambda A = B\phi'(0), \quad (7)$$

where ϕ' is the vertical (z) derivative of ϕ .

Multiplying equation (6) by $\phi'(0)$ and equation (7) by $\phi(0)$, and then equating, we can solve for A at $z = 0$ to give

$$E_2(0) = A = -E_1(0) \frac{(\phi'(0) + \lambda\phi(0))}{(\phi'(0) - \lambda\phi(0))}. \quad (8)$$

The electric field must decay at large values of z , so $\phi(z) \rightarrow 0$ as $z \rightarrow \infty$. Therefore, assuming a solution to equation (5) of the form

$$\phi(z) = e^{-\lambda z} f(z, \omega, \lambda), \quad (9)$$

equation (8) becomes

$$\frac{\lambda\phi(0)+\dot{\phi}(0)}{\lambda\phi(0)-\dot{\phi}(0)} = \frac{f'}{2\lambda f-f'} \Big|_{z=0} = K(\omega, \lambda, z) \Big|_{z=0}, \quad (10)$$

where $K(\omega, \lambda, z)$ is the kernel function introduced as a shorthand for the middle term in equation (10).

Substituting equation (10) into equation (8) and dropping the subscript 2 on the secondary field, we get

$$E(0) = - E_1(0)K(\omega, \lambda, 0). \quad (11)$$

For a step-function waveform $I(\omega) = 1/i\omega$, equation (4) in combination with equation (11) after the appropriate inverse Fourier and Hankel transforms can be used to give an expression for the secondary E -field time-domain response

$$E(r, z, t) = \frac{1}{2}\mu_0 a I_0 \int_0^\infty J_1(\lambda a) J_1(\lambda r) e^{-\lambda|h+z|} \frac{1}{2\pi} \int_{-\infty}^\infty e^{-i\omega t} K(\omega, \lambda, 0) d\lambda d\omega. \quad (12)$$

Differentiating equation (12) in accordance with equations (2) and (3), the radial and vertical components of the magnetic field can be written

$$H_j(t) = \frac{1}{2} a I_0 \int_0^\infty J_1(\lambda a) J_l(\lambda r) \lambda e^{-\lambda|h+z|} \frac{1}{2\pi} \int_{-\infty}^\infty \frac{1}{i\omega} e^{-i\omega t} K(\omega, \lambda, 0) d\lambda d\omega, \quad (13)$$

where the subscript indices are $j = r$, and $l = 1$ for the r -component and $j = z$, and $l = 0$ for the z -component. In deriving the z -component in equation (13), equation 9.1.30 of Abramowitz and Stegun (1972) is used for the r derivative of the Bessel function to give the zeroth-order Bessel function J_0 . The inverse Fourier transform in equation (13) will be evaluated using the residue theorem (Appendices A and B).

Using equation (B5) of Appendix B, the kernel in the inverse Fourier transform can be rewritten as

$$- K(\omega, \lambda, 0) = R_E(\lambda) \sum_{n=1}^\infty \frac{1}{s-\lambda_n} + \frac{1}{\lambda_n}, \quad (14)$$

where λ_n is the location of the n th pole of the left-hand side and $R_E(\lambda)$ is the residue defined in equation (A21). Hence, the inverse Fourier transform in equation (13) can be written

$$\begin{aligned} \frac{1}{2\pi} \int_{-\infty}^{-\infty} -\frac{1}{s} e^{-st} K(\omega, \lambda, 0) ds &= -\frac{1}{2\pi} \int_{-i\infty}^{-i\infty} \frac{1}{s} e^{-st} R_E \sum_{i=1}^{\infty} \left[\frac{1}{\lambda_i - s} - \frac{1}{\lambda_i} \right] ds \\ &= \frac{1}{2\pi} \int_{-i\infty}^{-i\infty} e^{-st} R_E \sum_{i=1}^{\infty} \left[\frac{1}{\lambda_i(s-\lambda_i)} \right] ds, \end{aligned} \quad (15)$$

where $s = i\omega$. The above equation can be evaluated using contour integration, which we chose to do using ω as the integration variable. The contour of integration is closed by a semicircle in the lower ω plane. In the lower semicircle, $e^{-i\omega t}$ approaches zero for large ω and Jordan's lemma tells us there is no contribution from this semicircle to the integral. The integral is thus the sum of the residues at the poles. As the poles are in the lower ω half-plane, then the real part of s is positive. In Appendix D, we also demonstrate that s is purely real, so the result is thus a sum of the decaying exponentials that are associated with each pole. Thus, substituting from equation (15) into equation (13), the magnetic field components are given by

$$H_j(t) = \frac{1}{2} a I_0 \int_0^{\infty} J_1(\lambda a) J_l(\lambda r) \lambda e^{-\lambda|h+z|} R_E(\lambda) \sum_{i=1}^{\infty} (e^{-\lambda_i t} - 1) / \lambda_i d\lambda, \quad (16)$$

where the values of j and l are given below equation (13) for the respective component. This magnetic field step response can be used to calculate the n th moment of the magnetic-field step response using the moment formula

$$M^n = \int_0^{\infty} t^n H(t) dt. \quad (17)$$

The impulse-response moments, M^n , of equation (1) are related to the step-response moments, M^n , in equation (17) via the relation

$$M^n = -nM^{n-1}, \quad (18)$$

which can be verified by integration by parts.

The moment integrals have lower and upper limits of zero and infinity, but it is also possible to calculate partial moments, with different limits to enhance certain parts of the decay. The following analysis could be undertaken using different limits, if desired. Alternatively, finite limits could be used for calculation of moments from field data and zero and infinity could be used for the limits for the theoretical moments, but this will result in some inaccuracy.

The step-response moment integrals $\int_0^{\infty} H(t)t^n dt$ can be evaluated inside the Hankel (λ) integral of equation (16) using the expression

$$\sum_{i=1}^{\infty} \int_0^{\infty} \frac{e^{-\lambda_i t}}{\lambda_i} t^n dt = n! \sum_{i=1}^{\infty} \frac{1}{\lambda_i^{n+2}}, \quad (19)$$

which can be proved by induction.

The time-independent $1/\lambda_i$ term in the sum in equation (16) is ignored as off-time EM methods typically only record the transient response.

Introducing the coefficients, β_j , defined in equation (E3) of Appendix E to rewrite equation (19), we get an R_E in the denominator, so when calculating the moments using equations (16), the R_E cancel and the formulae for the moments become

$$M_j^n = -\frac{1}{2} a I_0 n! \int_0^{\infty} J_1(\lambda a) J_l(\lambda r) \lambda e^{-\lambda|h+z|} \beta_{n+1} d\lambda, \quad (20)$$

and once again the values of j and l are given below equation (13) for the respective component.

Computation of moments using equation (20) involves evaluation of a Hankel integral, as discussed below. Higher-order moments require the calculation of β_n for larger values of n . As shown in Appendix E, the β_n coefficients are dependent on the manner that the conductivity varies as a function of depth. Up until now, the depth variation has not been specified, so these equations are general and could be applied to any depth variation with any functional form.

Theory for Gaussian conductivity function

As a specific example of the general procedure, we select a Gaussian conductivity depth function with maximum conductivity A_0 (S/m) at some depth $z = c$, viz.,

$$\sigma(z) = A_0 e^{-b(z-c)^2}, \quad (21)$$

where b (m^{-2}), is the parameter that controls the narrowness of the conductive zone or the rate of gradual decrease (and increase) of the conductivity. This function can approximate the conductivity variation in many real situations, e.g. where the salinity increases gradually to a maximum at some depth (Lee and Ignatik, 1994) and then decreases, or where the intensity of weathering decreases gradually with depth.

In order to calculate the zeroth and first order step response moments, we need to determine the coefficients β_1 and β_2 . Formulae have been derived in Appendix E for β_1 and β_2 in terms of functions f_1 and f_2 and their depth derivatives, evaluated at $z = 0$.

The procedure for calculating the moments for a Gaussian conductivity distribution is as follows:

- 1) Select the values of A_0 , b and c that define the desired conductivity.
- 2) Calculate f_1 using equation (F9), f_1' using equation (F5), and f_2' using equation (F17). Note that each of these functions must be evaluated for each value of λ in equations (F9), (F5) and implicitly in the I function in equation (F17).
- 3) Calculate the β_1 , β_2 and higher-order terms using equations (E14), (E15) and (E13) respectively.
- 4) Calculate the moments, using equation (20). The Hankel integrals in these equations have been calculated with the python routine `HankelTransform.integrate` (Murray, 2017), which is an implementation of the routine described by Ogata (2005). These calculations, can be sped up by invoking the small argument approximation so that $J_1(\lambda a) = \lambda a/2$ (Abramowitz and Stegun, 1972, equation 9.1.7)

Results for selected Gaussian conductivity models

As an example, we have calculated the moments for a Gaussian conductivity-depth profile with a range of b and c values and compared these with moments calculated using previously published formulae for a thin sheet, half-space and thin sheet

Thin sheet

In order to approximate a thin sheet with the Gaussian depth variation, we have chosen the thickness of the conductive part to decrease as the depth c decreases, so numerically we somewhat arbitrarily set $c = 1/b$ where the inserted value of b has units of inverse metres. The conductivity as a function of depth for four sets of c and b values are shown on Figure 1. The full width of the conductivity peak at half maximum can be determined from equation (21) to be $2\sqrt{\frac{\ln 2}{b}}$.

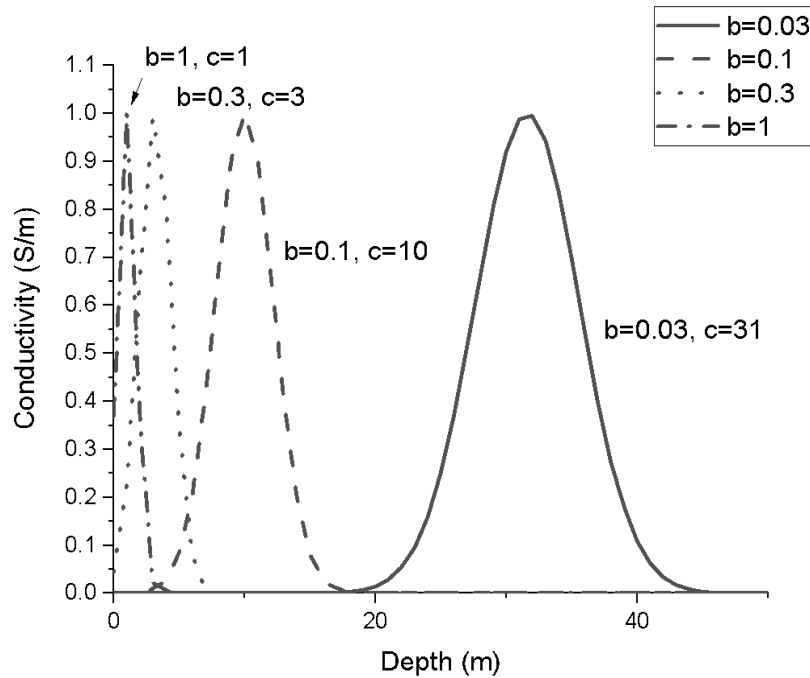


Fig. 1. Conductivity as a function of depth for four Gaussian functions with different decay constants, b , and centre depth $c = 1/b$. The cases with the narrowness parameter b large and c small (e.g. $b = 1$ and $c = 1$) approximate thin sheets near surface, but those with b small and c large represent thicker layers at greater depth. In all cases $A_0 = 1$ (S/m).

Smith and Lee (2002b) equations 49 to 52 can be used to calculate the zeroth- and first-order thin-sheet moments. Their moments were the impulse-response moments, and ours are the step-response moments, so we have added an additional factor of 2 in the denominator for the first moment, since from equation (18), $M^1 = -M^2/2$. As well, Smith and Lee (2002b) had h positive and z negative above the ground, but in this paper h and z are both positive as they are heights of the transmitter and receiver above the ground. Hence the $z - h$ in Smith and Lee (2002b) becomes $z + h$ here. Also, the depth c of the peak conductivity means that both z and h in the thin sheet formulae increase in magnitude by c . The formulae of Smith and Lee (2002b) include a conductance. The conductance value we use for the thin sheet is the conductance of the corresponding Gaussian function, which is calculated from equation (F8), after multiplying both sides by $2\lambda/\mu$.

In the following we assume $z = 70$ m and $h = 120$ m, while $r = 130$ m, which are the geometric parameters of the MEGATEM system (Smith et al., 2003b). For simplicity we assume a dipole moment of unity ($a^2 I_0 = 1$).

The zeroth-order moments calculated using the Gaussian conductivity variation and the thin-sheet formula are shown on Figure 2 for 13 values of the narrowness parameter, b . The black lines are the z component and the grey lines are the radial r component. The thin-sheet approximation works well for the narrowness parameter $b > 0.001$. The corresponding first-order moments are shown in Figure 3, in this case, the thin sheet approximation is reasonable for $b > 0.01$. Because the layers are relatively thick for b small, we do not expect the Gaussian and thin sheet formulae to agree, but the agreement in the limit of b large engenders confidence in the Gaussian formula for b large. For broader conductivity depth dependences, the Gaussian model with b small is more appropriate. Note that for the first-order moments (Figure 3), the thin-sheet assumption is valid for a smaller range of b values, so the Gaussian model is more appropriate for gradual variations in conductivity for this higher moment.

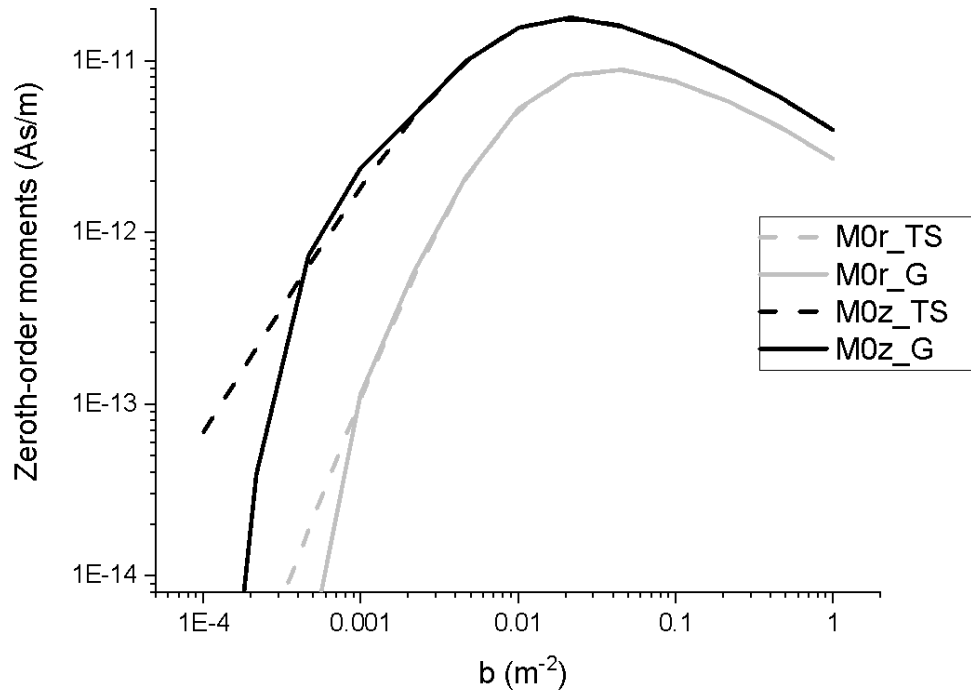


Fig. 2. The zeroth-order step-response moments (M_0) for Gaussian conductivity models with peak conductivity $A_0 = 1$ S/m, peak depth given by $c = 1/b$ m and the narrowness parameter or b values are given on the horizontal axis. The solid lines (_G) are calculated for the Gaussian model using equation (20) and the dashed lines are when we approximate the moments with a thin sheet model (_TS). Black is for the z -component moments and grey is for the radial r -component moments.

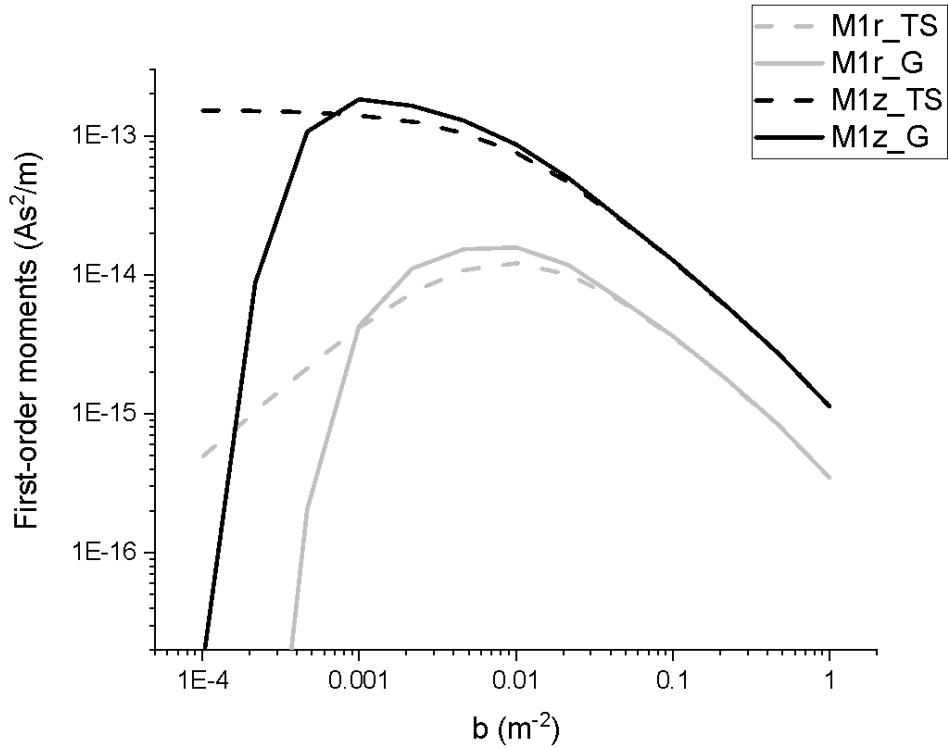


Fig. 3. The first-order step-response moments (M1) for conductivity variations parameterized by peak conductivity $A_0 = 1$, peak depth $c = 1/b$ and the narrowness parameter or b values are given on the horizontal axis. The solid lines for the Gaussian model (_G) are calculated using equation (20) and the dashed lines are when we approximate the moments with a thin sheet (_TS). Black is used for the z-component moments and grey is for the radial r -component moments.

Half-space

The uniform half-space violates the finite conductance condition, but if we chose broad or wide depth dependences (b small) and set $c = 0$ then a thick-layer approximates a half-space. Figure 4 shows conductivity-depth variations for seven values of b . When $b = 10^{-6} \text{ m}^{-2}$ the conductivity is almost constant above 100 m, but for larger b , the models look less like a half-space.

The zeroth-order moments for a half-space with conductivity σ are given in equations 58 and 59 of Smith and Lee (2002b), where, as above, modifications have been made to account for the different sign convention for heights of the transmitter and receiver. For zero-order moments, equation (18) tells us that $M^0 = -M^1$. For the half-space, the first- and higher-order step-response moments are not defined. However, for the Gaussian model, they are.

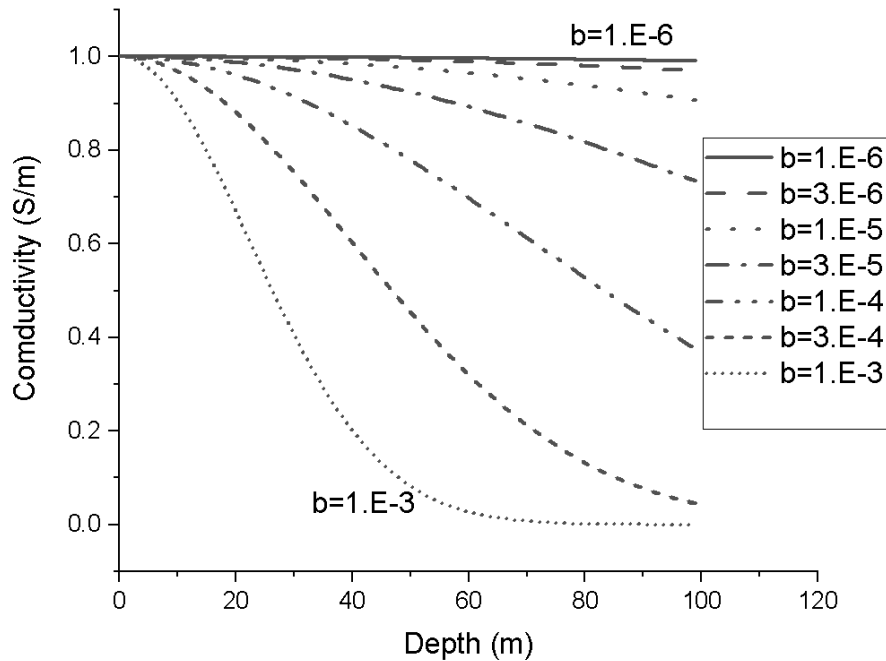


Fig. 4. Half-Gaussian conductivity curves, with the peak value $A_0 = 1$ (S/m) occurring at the ground surface, for seven narrowness parameters, b . The transmitter radius and current are unity, and the transmitter height, h , receiver height, z , and radial transmitter-receiver offset ρ are given by $h = 120$ m, $z = 70$ m and $\rho = 130$ m.

Moments for the half-Gaussian models in Figure 4 are plotted in Figure 5. The zeroth-order moments (solid lines) asymptote towards the half-space moments (dashed lines) for very small values of the narrowness parameter b , as we expect. This demonstrates that the zeroth-order moments when b is small (similar to a half-space) calculated using equation (20) are similar to those of a half-space. Because the integrals for the first-order moments for a half-space do not exist mathematically, this half-space example cannot be used to check equation (20) and the numerical implementation of the first-order moments for small b . However, equation (20) has been checked in the thin-sheet case discussed above. This example demonstrates that for very small values of b , the Gaussian model can be used to calculate first-order moments of conductivity structures that are very similar to a half-space (e.g., those on Figure 4 with b small), even though an ideal half-space does not have a first-order step-response moment. The strong variation in the first-order moment with b in Figure 5, implies that this moment is sensitive to b and could be used to accurately estimate b . Hence, if we use the first-order moments for interpreting data then it may be possible to discriminate a half-space from a Gaussian model with a very small value of b .

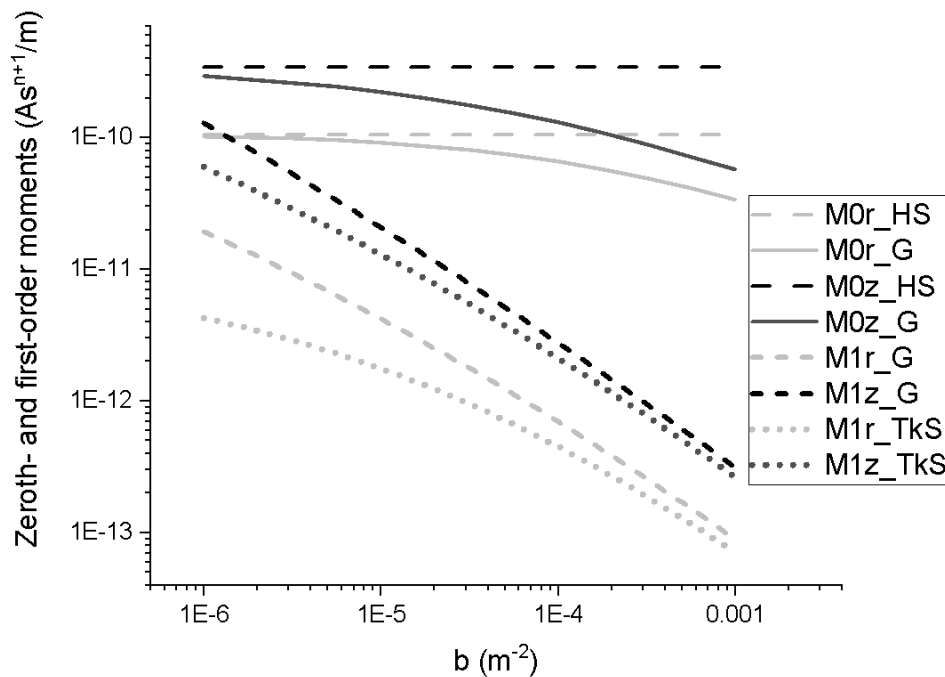


Fig. 5. The zeroth- (M0) and first-order (M1) step-response moments. The black and grey lines are the z and r components respectively. The half-Gaussian conductivities (ρ_G), calculated using equation (20) are when the conductivity decreases from a peak conductivity, $A_0 = 1$ (S/m), at the surface ($c = 0$) at a rate governed by the narrowness parameter, b , values shown on the horizontal axis. The solid lines are the zeroth-order moment and the short dashed lines are the first-order moment. The zeroth-order Gaussian moments are compared with the moments for a 1 S/m half-space (ρ_{HS}), shown with the long dashed lines. The first-order Gaussian moments are compared with the moments of a thick sheet (ρ_{Tks}) with thickness $d = \sqrt{\frac{\ln \ln 2}{b}}$, shown with dotted lines.

Thick sheet

As a further check on the theory, we can use the zeroth-order moment expressions for a thick sheet (layer) of thickness d , given in equations 30 and 31 of Smith and Lee (2002b), suitably modified as discussed previously.

Each of the conductivity distributions in Figure 4 can be approximated as a thick sheet with a thickness equal to the depth $d = \sqrt{\frac{\ln \ln 2}{b}}$, where the conductivity drops to half the value at the ground surface. The zeroth-order moments of the relevant approximate thick sheet, compared with the zero-order moment of the distributions shown in Figure 4 have the moments shown in Figure 6 using dashed lines. It can be seen that the approximate thick-sheet moments and the moments of the Gaussian distribution agree well, particularly for small values of the narrowness parameter b (which correspond to large values of the depth, d), where the model is essentially a half-space to great depth and for larger values of b (which correspond to small values of d), where the model is essentially a thin sheet at surface. In between these two limits, the agreement between the Gaussian and the thick sheet is also close, so for the zeroth-order

moment, the thick sheet is a reasonable approximation to the Gaussian case, but for higher-order moments, the behavior will be different, as we see below.

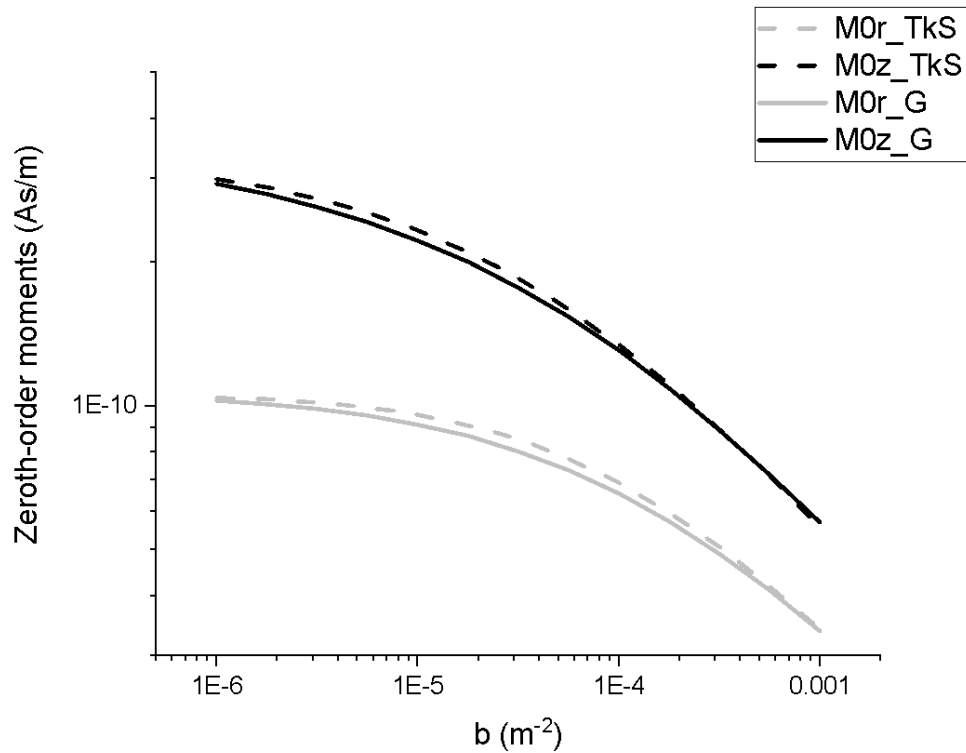


Fig 6. The zeroth-order step-response moments (M_0) for half-Gaussian conductivity variations parameterized by the peak conductivity $A_0 = 1$, peak depth, $c = 0$ and the narrowness parameter, b , values given on the horizontal axis. The solid lines for the Gaussian model ($_G$) are calculated using equation (20) and the dashed lines are when we approximate the moments with a thick sheet ($_TkS$) with thickness $d = \sqrt{\frac{\ln \ln 2}{b}}$. Black is the z -component moment and grey is the radial r -component moment.

The first-order moments for a thick sheet are given by the expressions in equations 40 and 43 of Smith and Lee (2002b), after modification as specified above. The first-order moments for the same thick sheets and half-Gaussian models as shown in Figure 6 are plotted in Figure 5 using dotted lines. For small values of b (close to a half-space), the moments for the half-Gaussian cases (solid lines) are up to a factor of five

greater than the thick sheet (dotted lines). Even for large values of b , corresponding to narrower cases there is still a 10 to 20% discrepancy between the Gaussian cases and the thick sheet. The increasing difference from zeroth to first-order moments suggests that for even higher-order moments the differences will be even greater. Hence it is important to have a means to calculate the higher-order moments, both for the Gaussian conductivity model and potentially other models. The increasing differences for the higher-order moments suggests that one or more higher-order moments might be used to more confidently identify gradual changes in conductivity with depth.

Discussion

The four formulae derived here for the zeroth- and first-order moments for the r and z components enable generation of maps of A_0 , b and c from airborne electromagnetic data. These parameters could characterize gradual variations of conductivity within the overburden. These characterizations would provide information that compliments the simple conductance or conductivity maps of Smith and Lee (2002b). Determination of A_0 , b and c involves non-linear inversion and is described in Smith and Lee (2020, submitted to Exploration Geophysics).

Our examples have been for the zeroth- and first-order moments of the magnetic field, but with additional effort, formulae for higher-order moments could be derived.

The example given above is for a Gaussian depth dependence, but other functional forms different from equation (21) could be derived if required, as long as: i) the integrated conductance is finite, and ii) the conductivity can be integrated [equation (E8)].

The zeroth-order moments alone are particularly important for resistive areas where the resistive-limit on-time response is measurable, but the off-time response is too small to measure (Annan et al., 1996;

Smith, 2001). The z - and r -component data represent only two measurements, and hence allow only two geoelectrical parameters to be determined, for example the conductivity or conductance and the depth. Or, if one parameter can be assumed, then perhaps the thickness or basement conductivity could be estimated (Bagley and Smith, 2018). The Gaussian model, provides other alternate parameters that can be estimated, for example, we could assume $c = 0$ and then determine A and b . This could avoid the difficult choice of deciding, for example, whether the thin-sheet or the half-space model is more appropriate, as a large narrowness parameter b would represent a thin sheet, a small b a half-space and intermediate b , would represent thicker sheets.

To illustrate the transition from the thin- to the thick-sheet models, the zeroth-order moments from the Gaussian models used to generate Figure 5 were used to estimate the half-space apparent conductivity and the thin-sheet apparent conductance. If the half-space model is appropriate, then the z - and r -component estimates will be consistent. This is quantified with a dimensionless consistency factor C , where

$$C = 1 - \left| \frac{\sigma_z - \sigma_r}{\sigma_z + \sigma_r} \right|, \quad (22)$$

where $| \cdot |$ denotes the absolute value. This consistency factor can be calculated for the thin sheet and half-space estimates, where σ_i is the apparent conductance for the thin-sheet case and the apparent conductivity for the half-space case. If the two estimates are consistent, $C = 1$, but if they are inconsistent, then $C < 1$. Figure 7 shows that the half-space model is more consistent for $b < 10^{-6}$ ($d > 830$ m), while the thin-sheet model at surface is more appropriate for $b > 0.001$ ($d < 26$ m). The Gaussian model will be appropriate in the range between these extremes, i.e., $10^{-6} < b < 0.001$, thus illustrating how our new Gaussian model allows at to interpret a broader class of models than the half-space or thin sheet models alone.

Recent work by Bagley and Smith (2018) suggests that in some areas of the Athabasca basin, neither a thin-sheet, thick-sheet or half-space model (Smith and Lee, 2002b) is appropriate. Hence, the Gaussian model proposed here, that can handle all three cases, is a useful model.

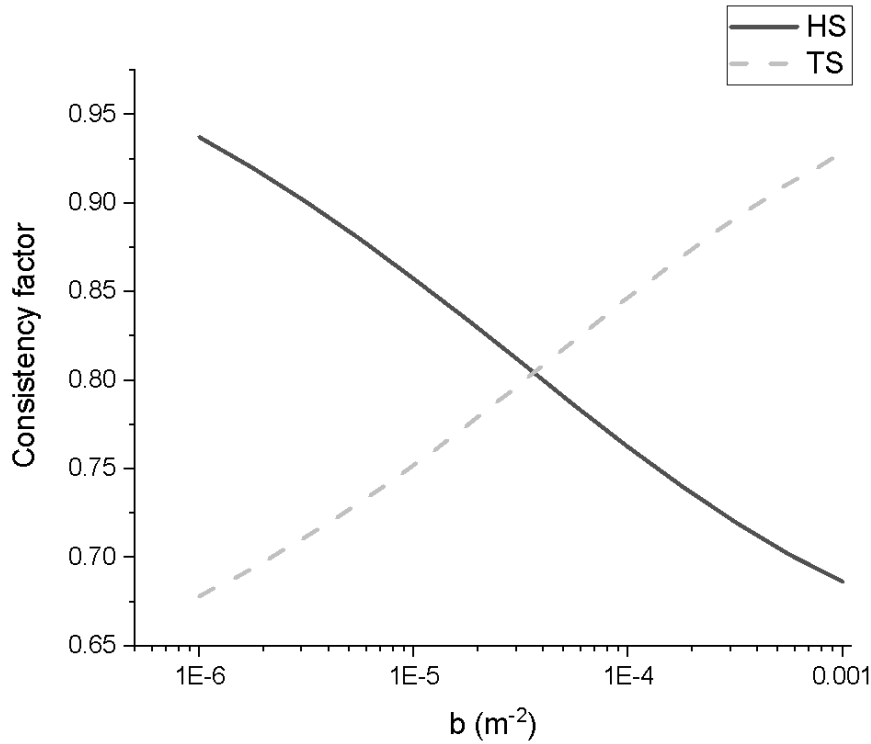


Fig. 7. Consistency factor for using the half-space (solid, HS) and thin-sheet (dashed, TS) models to approximate the Gaussian conductivity models shown in Figure 4. The parameter b is a measure of the narrowness of the model.

Conclusions

We have derived analytic expressions which enable us to calculate the step-response moments of the electromagnetic response of a vertically varying earth model. The moments can in principle be calculated for any moment order n , for a conductivity that varies as a function of depth in any fashion, provided that

it has finite conductance. For the general case, we have derived formulae for zeroth- and first-order moments. In principle, formulae for higher-order moments could be obtained with further effort.

The theory has been applied to the specific example of a Gaussian conductivity, $\sigma(z) = A_0 e^{-b(z-c)^2}$, that either decreases from the surface or defines a peak conductivity at some depth. For the Gaussian conductivity, analytic formulae for the moments have been derived in terms of the parameters A_0 , b , and c . For other conductivity functions the moments could be computed numerically.

The formula for the first-order step-response moment of the Gaussian model in the limit of small b allows a moment to be calculated for a model that is similar to a half-space. Previously, there was no formula for these first-order moments for the case of a half-space as the integral is unbounded for an infinite upper limit. The Gaussian moment formulae also apply to other cases, such as a conductivity increasing gradually with depth (small b and large c).

The formulae for higher-order moments allow more geoelectrical parameters to be derived from the measured data, for example, we can determine the parameters A_0 , c and b from three moments. This will be particularly useful in areas where the conductivity varies gradually with depth and the thin-sheet, thick sheet and half-space models are inappropriate. Further, in some survey areas a thin sheet might be appropriate to model the geoelectric structure in some parts and a half-space in another parts; however, the Gaussian model is flexible enough to suit a range of geoelectric sections, with appropriate choice of parameters.

We argue that for higher-order moments there was a stronger difference between gradual and sharp variations of conductivity with depth, so these higher-order moments could potentially be important in identifying these types of gradual variations.

In the past, maps of the conductance or conductivity have been derived from airborne electromagnetic data, but in the future, it will be possible to derive maps of other parameters, some of which quantify how rapidly the conductivity changes as a function of depth.

Acknowledgements

We are grateful to anonymous reviewers and Peter Fullagar, who greatly improved the clarity and quality of this manuscript. Richard Smith is grateful to an NSERC Discovery Grant for supporting this work.

Appendix A - Calculation of the residues

In this appendix we look at the residues of the kernel function $K(\lambda, \omega, 0)$ defined in equations (10) and used in equation (13).

Using $k_1^2 = \mu\sigma s$, and using a prime symbol ' to denote a differentiation w.r.t. z , equation (5) becomes

$$\phi'' - \lambda^2 \phi + \mu\sigma\phi = 0. \quad (\text{A1})$$

We now investigate the behaviour of the solution as a function of frequency, by differentiating with respect to the Laplace transform variable $s = i\omega$.

$$\phi_s'' - \lambda^2 \phi_s + \mu\sigma\phi + \mu\sigma s \phi_s = 0, \quad (\text{A2})$$

where by definition

$$\phi_s = \frac{\partial\phi}{\partial s} = \frac{\partial\phi}{\partial i\omega}. \quad (\text{A3})$$

Multiplying equation (A2) by ϕ and equation (A1) by ϕ_s and then subtracting gives

$$\phi_s \phi'' - \phi \phi_s'' - \mu\sigma\phi^2 = 0. \quad (\text{A4})$$

Rearranging and integrating by parts

$$\int_z^{\infty} \mu \sigma \phi^2 dz = (\phi_s \phi' - \phi \phi'_s) \Big|_z^{\infty} - \int_z^{\infty} (\phi'_s \phi' - \phi \phi'_s) dz. \quad (A5)$$

The two terms in the integral on the extreme right-hand side cancel. The remaining terms are evaluated at infinity and z . Both $\phi(z) = e^{-\lambda z} f(z)$ and $\phi_s(z) = e^{-\lambda z} f_s(z)$ tend to zero as $z \rightarrow \infty$. Hence,

$$\int_z^{\infty} \mu \sigma \phi^2 dz = - [\phi(z) \phi'_s(z) - \phi(z) \phi'_s(z)]. \quad (A6)$$

In terms of f and f_s , equation (A6) can also be written

$$\int_z^{\infty} \mu \sigma e^{-2\lambda z} f^2 dz = - e^{-2\lambda z} (f'_s f - f f'_s) \quad (A7)$$

The zeros of equation (10) are when $f' = 2\lambda f$. Also, the middle quantity in equation (10) is in the form of a quotient $p(s)/q(s)$. If s_0 is a zero of $q(s)$ so that $q(s_0)=0$ and if the residue exists (established below) then the residue is $p(s_0)/q'_s(s_0)$, where the subscript s denotes the derivative w.r.t s (see for example Brown and Churchill (2004) equation 2, page 253).

Hence we get

$$Res \frac{f'(z)}{2\lambda f(z) - f'(z)} = \frac{f'(z)}{2\lambda f_s(z) - f'_s(z)}, \quad (A8)$$

where “Res” means residue of. If we multiply top and bottom of the right hand side by f and use $f' = 2\lambda f$ to eliminate a $2\lambda f$ on the denominator and a f' in the numerator, then we get an expression where we can use equation (A7) to give

$$Res \frac{f'}{2\lambda f - f'} = \frac{2\lambda f^2}{f'_s f - f f'_s} = \frac{2\lambda f^2}{-e^{-2\lambda z} \int_z^{\infty} \mu \sigma e^{-2\lambda z} f^2 dz}. \quad (A9)$$

This expression is independent of any particular root of $2\lambda f - f' = 0$, as the integral in the denominator on the right-hand side is evaluated in the same way regardless of how f_s is evaluated.

From the definition of $k_1^2 = \mu\sigma s$, then if the conductivity varies as a function of depth, so will k_1 , requiring that at a zero s is a function of z , as we demonstrate in what follows. At the poles we know that $2\lambda f - f' = 0$, which is of the form $g(s, z) = 0$. As g is dependent on two variables, we can use equation 4 from Brand (1960, p 160), viz.

$$dg = \frac{\partial g}{\partial s} ds + \frac{\partial g}{\partial z} dz . \quad (\text{A10})$$

But as $g(s, z) = 0$, which is a constant for all values of s and z , so g does not change, hence we know that $dg = 0$, so dividing both sides by dz , we get

$$0 = \frac{\partial g}{\partial s} \frac{ds}{dz} + \frac{\partial g}{\partial z} , \quad (\text{A11})$$

But the $\frac{ds}{dz}$ should be written as a partial derivative. Using the above equation, we can differentiate

$2\lambda f - f'$ to get at the zero

$$\left(2\lambda f_s - f'_s\right) \frac{\partial s}{\partial z} + (2\lambda f' - f'') = 0 . \quad (\text{A12})$$

Given equation (9) it follows from equation (5) that the function f must satisfy the differential equation

$$f'' - 2\lambda f' + k^2 f = 0 , \quad (\text{A13})$$

where we have dropped the subscript 1 for the k . This can be rewritten as $(2\lambda f' - f'') = k^2 f$, so equation (A12) becomes

$$\frac{\partial s}{\partial z} = \frac{-k^2 f}{(2\lambda f_s - f'_s)} . \quad (\text{A14})$$

Because s has a finite derivative w.r.t. z , then s must be a function of z . In a similar way, we can differentiate equation (A13) w.r.t z to give

$$f''' - 2\lambda f'' + \mu_0 \frac{\partial(k^2)}{\partial z} f + k^2 f' = 0. \quad (\text{A15})$$

However, at the poles we have $f' = 2\lambda f$, so $f'' = 2\lambda f'$ and similarly $f''' = 2\lambda f''$. This is because we allow k^2 to vary as a function of z and s so that $f' = 2\lambda f$. Then for varying z (and s), the other two expressions for f'' and f''' can be obtained by differentiation. Substituting these three expressions for the single, double and triple primed terms and using $k^2 = \mu_0 \sigma s$ gives

$$2\lambda(f'' - 2\lambda f' + k^2 f) + \mu_0 \frac{\partial(s\sigma)}{\partial z} f = 0 \quad (\text{A16})$$

The first term in brackets is zero [equation (A13)], and since f is non-zero at the pole, we can divide both sides by $\mu_0 f$ so using the product rule we get

$$\frac{\partial s}{\partial z} \sigma + s \frac{\partial \sigma}{\partial z} = 0, \quad (\text{A17})$$

and hence

$$\frac{\partial s}{\partial z} = -\frac{s}{\sigma} \frac{\partial \sigma}{\partial z}. \quad (\text{A18})$$

First we will calculate the residues when $\frac{\partial \sigma}{\partial z}|_{z=0 \neq 0}$. Combining equations (A14) and (A18), we have

$$\frac{\partial s}{\partial z} = \frac{k^2 f}{f'_s - 2\lambda f_s} = -\frac{s}{\sigma} \frac{\partial \sigma}{\partial z} \quad (\text{A19})$$

If we multiply throughout by $-2\lambda/k^2$ and use $f' = 2\lambda f$, then the middle term becomes the residual in equation (A8) that we are trying to evaluate at the location of the boundary condition, i.e., depth $z = 0$.

Hence

$$Res = -\frac{-f'}{f'_s - 2\lambda f_s} = \frac{2\lambda}{k^2} \frac{s}{\sigma} \frac{\partial \sigma}{\partial z} \Big|_{z=0} \quad (\text{A20})$$

Or using $k^2 = \mu_0 \sigma s$

$$Res = - \frac{-f'}{f_s' - 2\lambda f_s} = \frac{2\lambda}{\sigma^2 \mu} \frac{\partial \sigma}{\partial z} \Big|_{z=0}. \quad (A21)$$

This establishes that the residue exists, is defined and dependent on the conductivity at the surface and its derivative.

Second, we consider the case when $\frac{\partial \sigma}{\partial z} \Big|_{z=0} = 0$, which occurs for the $c = 0$ case. If $\frac{\partial \sigma}{\partial z} \Big|_{z=0} = 0$, then from equation (A18) $\frac{\partial s}{\partial z} \Big|_{z=0} = 0$. Hence, the numerator of the right-hand side of equation (A14) must be zero.

The electric field at the surface is non-zero, so from the definition of f at equation (9) and ϕ after equation (5), f cannot be zero at the surface. Hence, the other factor, in the numerator of equation (A14), k^2 , must be zero at the surface. Since $k^2 = \mu \sigma s$, and the σ is not zero at the surface for a Gaussian distribution, we can conclude that $s = 0$ at the surface. When $s = 0$, the differential equation for f [equation (A13)] implies that we can set f to a constant (as we argue below equation (E8) for the equivalent case of $\sigma = 0$). As f is now specified to be a constant, then for $z = 0$ the right-hand side of equation (A9) contains the conductance in the denominator, which we have assumed is finite. Hence the residue can be calculated from equation (A9), so we have the residue for this second case.

$$Res \frac{f'}{2\lambda f - f'} = - \frac{2\lambda}{s}. \quad (A9)$$

In other parts of the paper this residue Res defined on the right of equation (A22) or (A21) will be represented by the variable $R_E(\lambda)$.

Appendix B – Series expansion of the integral equation kernel

The expansion of the kernel in the Fourier integral of equation (13)

$$\frac{f'(s)}{f'(s)-2\lambda f(s)}, \quad (\text{B1})$$

requires that it be analytic everywhere except at the poles. The following analysis of this kernel follows Watson (1966, p 497). We begin by examining the integral

$$\frac{1}{2\pi i} \int_D \frac{s}{q(q-s)} \frac{f'(q)}{[f'(q)-2\lambda f(q)]} dq, \quad (\text{B2})$$

where s is any point within the rectangle D other than where $f'(q) - 2\lambda f(q) = 0$.

The integral in equation (B2) is different from that in equation (15), so we use a different contour of integration, D , which is the rectangle $\pm A, \pm iB$, where A and B are >0 . The only poles of the integrand inside the rectangle are at $q = s$ and the zeros of $f'(q) - 2\lambda f(q) = 0$. There is no residue associated with $q = 0$, as expanding the $f'(q)$ using the power series in q using equation (E7) gives a series with a common factor of q (given $f_0 = 1$, as per Appendix E). Hence the q in the denominator is not a pole because it cancels with the q in the numerator. As the zeros are simple (Appendix C), there is no other possibility for another residue. We now suppose that λ_n ($n=1, \dots, \infty$) are the zeros of $f'(q) - 2\lambda f(q) = 0$. The values of these zeros are yet to be determined. The residues associated with these zeros are obtained by writing the integrand of equation (B2) in the form $p(q)/g(q)$ and if q_0 is a zero of $g(q)$ so that $g(q_0) = 0$ and if $g_q(q_0) \neq 0$ and $p(q_0) \neq 0$, where the subscript q denotes a derivative of the function w.r.t. q , then the residue is $p(q_0)/g_q(q_0)$ (Brown and Churchill (2004) equation 2, p 253). At the pole $q = s$, the residue is $\frac{f'(s)}{f'(s)-2\lambda f(s)}$ because the pole is simple (Appendix C).

Then for A and $B \rightarrow \infty$ we can evaluate the integral using of the sum of the residue at $q = s$ plus those at $q = \lambda_n$.

$$\frac{1}{2\pi i} \int_D \frac{s}{q(q-s)} \frac{f'(q)}{f'(q)-2\lambda f(q)} dq = \frac{f'(s)}{f'(s)-2\lambda f(s)} + \sum_{n=1}^{\infty} \frac{s}{\lambda_n(\lambda_n-s)} \frac{f'(\lambda_n)}{[f'_q(\lambda_n)-2\lambda f'_q(\lambda_n)]} \quad (\text{B3})$$

$$= \frac{f'(s)}{f'(s)-2\lambda f(s)} + \sum_{n=1}^{\infty} \frac{f'(\lambda_n)}{f'_q(\lambda_n)-2\lambda f'_q(\lambda_n)} \left[\frac{1}{\lambda_n-s} - \frac{1}{\lambda_n} \right]. \quad (\text{B4})$$

Since we argued in Appendix A after equation (A9) that the residues were independent of any particular root, then the residues are the same for all λ_n , then we can assign this residue a specific value, R_E .

The integrand in the integral on the left hand side of equation (B3) is bounded along the boundary of the rectangle, so the integral goes to zero. Hence the right-hand side is equal to zero, so we can rearrange this to give

$$\frac{f'(s)}{f'(s)-2\lambda f(s)} = -R_E(\lambda) \sum_{n=1}^{\infty} \left[\frac{1}{\lambda_n-s} - \frac{1}{\lambda_n} \right] \quad (\text{B5})$$

The kernel function can thus be written as a sum involving the zeros.

Appendix C - Demonstration that all poles of the integral equation kernel are simple

This part of the appendix shows that zeros of $f' - 2\lambda f$ are simple. Start with equation (A13)

$$f'' - 2\lambda f' + k^2 f = 0. \quad (\text{C1})$$

Differentiate this equation w.r.t. s

$$f''_s - 2\lambda f'_s + k^2 f_s + \sigma \mu f = 0. \quad (\text{C2})$$

At a zero $s = i\omega$ is a positive real number [Appendix B and discussion after equation (15)]. Multiply equation (C1) by $e^{-2\lambda z} f_s$ and equation (C2) by $e^{-2\lambda z} f$

$$e^{-2\lambda z} f_s f'' - 2\lambda e^{-2\lambda z} f_s f' + e^{-2\lambda z} f_s^2 k f = 0, \quad (\text{C3})$$

$$e^{-2\lambda z} f f_s'' - 2\lambda e^{-2\lambda z} f f_s' + e^{-2\lambda z} f k f_s^2 + \sigma \mu e^{-2\lambda z} f f = 0. \quad (\text{C4})$$

Subtract these two and integrate w.r.t. z will give an expression that can be written

$$\int_z^\infty f_s \frac{\partial}{\partial z} \left(e^{-2\lambda z} f' \right) - f \frac{\partial}{\partial z} \left(e^{-2\lambda z} f_s' \right) dz = + \int_z^\infty \sigma \mu e^{-2\lambda z} f^2 dz. \quad (\text{C5})$$

Integrating by parts

$$\left(f_s e^{-2\lambda z} f' - f e^{-2\lambda z} f_s' \right) \Big|_z^\infty - \int_z^\infty f_s' e^{-2\lambda z} f' - f' e^{-2\lambda z} f_s' dz = + \int_z^\infty \sigma \mu e^{-2\lambda z} f^2 dz. \quad (\text{C6})$$

The first term has a zero contribution when evaluated at infinity; and the second term has a zero integrand. Hence, this simplifies to

$$- e^{-2\lambda z} \left(f_s f' - f f_s' \right) = \int_z^\infty \sigma \mu e^{-2\lambda z} f^2 dz. \quad (\text{C7})$$

Again, we use the constraint at a zero $f' = 2\lambda f$, so we get

$$e^{-2\lambda z} f \left(2\lambda f_s - f_s' \right) = - \int_z^\infty \sigma \mu e^{-2\lambda z} f^2 dz, \quad (\text{C8})$$

and as f and all other terms on the right are finite, so we can conclude that $\left(2\lambda f_s - f_s' \right) \neq 0$, so the zeros are simple.

Appendix D – Demonstration that all poles are located at real values of s

The denominator of equation (10) is important, so we investigate the zeros of $f'(z) - 2\lambda f(z)$ to establish that the zeros occur when s is real and positive.

From equation (A13) we know that $f'' - 2\lambda f' + k^2 f = 0$ for all z below the interface. If we let f^* be the complex conjugate of f , then the integral from some positive depth z to infinity of the right-hand side of equation (A13) multiplied by f^* must also be zero.

$$\int_z^\infty f^* (f'' - 2\lambda f') + k^2 f^* f dz = 0. \quad (D1)$$

Integrating the first term by parts gives an equation with three terms

$$f^* (f' - 2\lambda f) \Big|_z^\infty - \int_z^\infty f^{*'} (f' - 2\lambda f) dz + \int_z^\infty k^2 f f^* dz = 0 \quad (D2)$$

The first term has a multiplier f^* that is zero at the upper limit (infinity) because f and hence its complex conjugate goes to zero. Physically, this is because the fields go to zero for large z but mathematically, Morse and Feshbach (1953, pp. 1092-4) give an asymptotic expansion that shows we can choose such an f in this limit. The $(f' - 2\lambda f)$ in the first term is by definition zero as the lower limit (z) is the zero of the kernel function we are investigating. The first term is thus zero at both limits.

Splitting the second term into two, and assuming the quasi static limit, we have

$$- \int_z^\infty f^{*'} f' dz + 2\lambda \int_z^\infty f^{*'} f dz + \int_z^\infty \mu \sigma i \omega f f^* dz = 0 \quad (D3)$$

The first integral is the complex conjugate of the derivative multiplied by the derivative, so is purely real.

Since we are investigating the kernel function at the zero, then $f' - 2\lambda f = 0$, so we can use $f' = 2\lambda f$ and $f^{*'} = 2\lambda f^*$ to rewrite the second term to give

$$-\int_z^{\infty} f^* f' dz + 2\lambda \int_z^{\infty} 2\lambda f^* f dz + \int_z^{\infty} \mu \sigma i \omega f f^* dz = 0 \quad (\text{D4})$$

The first and second term each have a complex conjugate multiplied by itself, so they are both purely real. In order for all three terms to sum to zero, the third term must also be pure real, so $i\omega$ is real, and hence $s = i\omega$ is pure real at the zeros.

Appendix E – Analytic expressions for the coefficients β_n

From equation (20), the n th-order moments are expressed as Hankel transforms of the coefficients, $\beta_{n+1}(\lambda)$, analytic expressions for which are derived below.

Separating out the common factor $1/\lambda_n$ and applying the binomial series expansion (Abramowitz and Stegun, 1972, equation 3.6.10) it is possible to recast the right-hand-side of equation (14) as a series in s :

$$-K(\omega, \lambda, 0) = -R_E \sum_{n=1}^{\infty} \frac{1}{\lambda_n} \sum_{m=1}^{\infty} \frac{s^m}{\lambda_n^m} \quad (\text{E1})$$

Our analysis below uses a Taylor series expansion, which by definition uses an index n that starts at an index of $n = 0$ and hence we define some yet to be determined $\beta_n(\lambda)$ such that

$$-K(\omega, \lambda, 0) = \sum_{n=0}^{\infty} \beta_n s^n = -R_E \sum_{n=1}^{\infty} \frac{1}{\lambda_n} \sum_{m=1}^{\infty} \frac{s^m}{\lambda_n^m} . \quad (\text{E2})$$

However, for this particular expansion, by inspection we can see that we have $\beta_0 = 0$. Expanding the right-hand side and once equating like powers we can show

$$\beta_j = -R_E \sum_{n=1}^{\infty} \frac{1}{\lambda_n^{j+1}} , \quad \text{for } j \geq 1 \quad (\text{E3})$$

In order to determine the coefficients, β_n , in equation (E2), we return to equation (A13) and integrate term by term to give

$$f' - 2\lambda f = \int_z^{\infty} k^2 f dz', \quad (\text{E4})$$

using the fact that f and f' is zero at infinite z . Multiplying throughout by $e^{-2\lambda z}$,

$$\begin{aligned} e^{-2\lambda z} f' - 2\lambda e^{-2\lambda z} f &= e^{-2\lambda z} \int_z^{\infty} k^2 f dz', \\ \frac{\partial}{\partial z} (e^{-2\lambda z} f) &= e^{-2\lambda z} \int_z^{\infty} k^2 f dz'. \end{aligned} \quad (\text{E5})$$

Both sides of equation (E5) are now integrated from z to infinity. The left-hand side reduces to $-e^{-2\lambda z} f$ since the limit at infinity is zero. The right-hand side is integrated by parts, using the $e^{-2\lambda z}$ as the derivative. This gives

$$-e^{-2\lambda z} f = \frac{1}{2\lambda} e^{-2\lambda z} \int_z^{\infty} k^2 f dz' - \frac{1}{2\lambda} \int_z^{\infty} e^{-2\lambda z'} k^2 f dz'. \quad (\text{E6})$$

From examination of equation (E1) it can be inferred that f admits a series expansion of the form

$$f(z, s) = \sum_{n=0}^{\infty} f_n(z) s^n. \quad (\text{E7})$$

Substituting equation (E7) into equation (E6) and equating like powers of s yields a recursion relation between f_n and f_{n-1} :

$$f_n(z) = -\frac{1}{2\lambda} \int_z^{\infty} \sigma \mu f_{n-1} dz' + \frac{1}{2\lambda} e^{+2\lambda z} \int_z^{\infty} \sigma \mu e^{-2\lambda z'} f_{n-1} dz'. \quad (\text{E8})$$

All coefficients, f_n , can be determined from (E8) if we know the zeroth-order coefficient, f_0 . For the case when $\sigma = 0$, both terms on the right of equation (E8) are zero, so all the higher-order coefficients are zero and the series degenerates to the zeroth-order term only. Hence, if we can find the zeroth-order term for zero conductivity, then, we have the zero-order coefficient for all cases and can use this to calculate the

higher-order coefficients for all cases. For $\sigma = 0$, the differential equation (A13) simplifies to

$f'' - 2\lambda f' = 0$. The solution to this equation is of the form $f = Ce^{2\lambda z} + D$, where C and D are local constants to be determined. Since $e^{2\lambda z} \rightarrow \infty$ while $z \rightarrow \infty$ is not a possible solution, the only possible solution has $C = 0$ and, so $f = D$. For simplicity, we can set $f = 1$. If we chose a different value, then the value of B in equations (6) and (7) would be different. However, there would be no difference in the final result, as the value of B has cancelled when the kernel function is calculated using equation (10). As we use $f = 1$ below, then this means that we will use $f' = 0$ in the discussion of the poles after equation (B2) as they both relate to the case when $\sigma = 0$. Since we have selected $f = 1$, for the case $\sigma = 0$, this selection can also be used for all cases and it determines the first term in the series expansion, $f_0 = 1$. For all other cases ($\sigma \neq 0$) other f_n in the expansion will be non-zero. The first coefficient is

$$f_1(z) = -\frac{1}{2\lambda} \int_z^\infty \sigma \mu f_0 dz' + \frac{1}{2\lambda} e^{+2\lambda z} \int_z^\infty \sigma \mu e^{-2\lambda z'} f_0 dz' . \quad (\text{E9})$$

We are evaluating the series expansion for f at the upper interface, $z = 0$, so equation (E9) simplifies to

$$f_1(z)|_{z=0} = -\frac{1}{2\lambda} \int_z^\infty \sigma \mu (1 - e^{-2\lambda z'}) dz' . \quad (\text{E10})$$

More generally,

$$f_n(z)|_{z=0} = -\frac{1}{2\lambda} \int_z^\infty \sigma \mu (1 - e^{-2\lambda z'}) f_{n-1} dz' . \quad (\text{E11})$$

From this equation, we can see that the f_0 is an arbitrary scaling factor applied to all f_n , which is consistent with our argument for setting $f_0 = 1$. Using a non-zero value ensures that there is a secondary field present for all conductivities.

We also require a recursion relation for f_n' , obtained by differentiating equation (E8) with respect to z .

The derivative of the integral in the first term returns the negative of the integrand (as z is the lower limit), and the second term is differentiated using the product rule. The result simplifies to

$$f'_n(z)|_{z=0} = \int_z^\infty \sigma(z') \mu e^{-2\lambda z'} f_{n-1} dz', \quad (\text{E12})$$

when $z = 0$. Substituting $f' = \sum_{n=0}^{\infty} f'_n s^n$ and $f = \sum_{n=0}^{\infty} f_n s^n$ into the kernel function of equation (E2) that is

defined in equation (10), and equating the terms containing s^n gives

$$f'_n(0) = \sum_{i=0}^n \beta_{n-i} \left(f'_i(0) - 2\lambda f_i(0) \right). \quad (\text{E13})$$

For $n = 1$, given $\beta_0 = 0$, $f'_0 = 0$ and $f_0 = 1$, it follows from (E13) that

$$\beta_1(\lambda) = \frac{-f'_1(0)}{2\lambda}. \quad (\text{E14})$$

For the $n = 2$ case we obtain

$$\beta_2(\lambda) = \frac{-f'_2(0)}{2\lambda} - \frac{f'_1(0)}{4\lambda^2} \left(f'_1(0) - 2\lambda f_1(0) \right). \quad (\text{E15})$$

A similar procedure can be used to determine β_3 and higher order coefficients. However, the analytic formulae become more complicated as n increases, so for higher-order moments it may be more practical to calculate the f_n and f'_n by numerically integrating equations (E11) and (E12).

Appendix F - Calculation of $f'_1(0)$, $f_1(0)$ and $f'_2(0)$ for the Gaussian conductivity function

To determine $f'_1(0)$ we define an integral as $I(z, c, \lambda)$, where the argument z is the lower limit of integration

$$I(z, c, \lambda) = \mu A_0 \int_z^\infty e^{-b(z'-c)^2} e^{-2\lambda z'} dz', \quad (\text{F1})$$

and the functional dependence of $I(z, c, \lambda)$ on λ is henceforth implied. Substituting equation (21) into (E12) with $n = 1$ and $f_0 = 1$, it can be verified that $I(0, c) = f_1'(0)$. Re-arranging the exponentials in equation (F1) gives

$$I(z, c) = \mu A_0 e^{-\lambda(2c - \frac{\lambda}{b})} \int_z^{\infty} e^{-b(z' - (c - \frac{\lambda}{b}))^2} dz'. \quad (F2)$$

If we now make the substitution $w = \sqrt{b}(z' - c + \frac{\lambda}{b})$, then $dw = \sqrt{b}dz'$; and at $z' = z$ we have

$w = \sqrt{b}(\frac{z+\lambda}{b} - c)$, so

$$I(z, c) = \mu A_0 e^{-\lambda(2c - \frac{\lambda}{b})} \frac{1}{\sqrt{b}} \int_{\sqrt{b}(\frac{z+\lambda}{b} - c)}^{\infty} e^{-w^2} dt, \quad (F3)$$

from which we can use the definition of the complimentary error function to write

$$I(z, c) = \mu A_0 e^{-\lambda(2c - \frac{\lambda}{b})} \frac{1}{\sqrt{b}} \frac{\sqrt{\pi}}{2} \operatorname{erfc}\left(\sqrt{b}\left(\frac{z+\lambda}{b} - c\right)\right). \quad (F4)$$

Setting $z = 0$, we obtain the desired result

$$f_1'(0) = \mu A_0 e^{-\lambda(2c - \frac{\lambda}{b})} \frac{1}{\sqrt{b}} \frac{\sqrt{\pi}}{2} \operatorname{erfc}\left(\sqrt{b}\left(\frac{\lambda}{b} - c\right)\right). \quad (F5)$$

In order to calculate f_1 at $z = 0$, we rewrite equation (E9) in the form

$$f_1(0) = -\frac{1}{2\lambda} \int_0^{\infty} \sigma \mu dz' + \frac{1}{2\lambda} \int_0^{\infty} \sigma \mu e^{-2\lambda z'} dz'. \quad (F6)$$

The second integral can be recognized from equation (E12) as f_1' evaluated at $z = 0$, hence

$$f_1(0) = -\frac{1}{2\lambda} \int_0^{\infty} \sigma \mu dz' + \frac{1}{2\lambda} f_1'(0) \quad (F7)$$

Focusing on the first integral on the right-hand-side of (F7) for a Gaussian conductivity variation as per (21), we get

$$\frac{1}{2\lambda} \int_0^{\infty} \sigma \mu dz' = \int_0^{\infty} \frac{\mu A_0 e^{-b(z'-c)^2}}{2\lambda} dz' = \frac{\mu A_0}{2\lambda\sqrt{b}} \frac{\sqrt{\pi}}{2} \operatorname{erfc}(-c\sqrt{b}), \quad (\text{F8})$$

where the right-hand-side is obtained using 7.4.2 from Abramowitz and Stegun (1972). Equations (F8) and (F5) can be substituted into equation (F7) to give

$$f_1(0) = -\frac{\mu A_0}{2\lambda\sqrt{b}} \frac{\sqrt{\pi}}{2} [(c\sqrt{b}) + 1] + \frac{1}{2\lambda} \mu A_0 e^{-\lambda(2c-\frac{\lambda}{b})} \frac{1}{\sqrt{b}} \frac{\sqrt{\pi}}{2} \operatorname{erfc}\left(\sqrt{b}\left(\frac{\lambda}{b} - c\right)\right), \quad (\text{F9})$$

where $\operatorname{erfc}(-c\sqrt{b}) = (c\sqrt{b}) + 1$ (Abramowitz and Stegun, 1972). This is the desired analytic formula for $f_1(0)$.

Equation (E12) is used with $n = 2$ to evaluate f_2' at $z = 0$,

$$f_2' \Big|_{z=0} = \int_z^{\infty} \sigma(z') \mu e^{-2\lambda z'} f_1' dz'. \quad (\text{F10})$$

Integrating by parts gives

$$f_2' \Big|_{z=0} = f_1'(z) \int_z^{\infty} \sigma(z_2) \mu e^{-2\lambda z_2} dz_2 \Big|_{z=0} - \int_z^{\infty} \left[\frac{df_1(z')}{dz'} \right]_{z_2=z'} \int_{z_2=z'}^{\infty} \sigma(z_2) \mu e^{-2\lambda z_2} dz_2 dz'. \quad (\text{F11})$$

The integral in the first term is of the form of the integral in equation (F1), which can by definition be written as $I(z, c)$. Thus

$$f_2' \Big|_{z=0} = f_1'(z) I(z, c) \Big|_{z=0} - \int_{z=0}^{\infty} \int_{z_2=z}^{\infty} \sigma(z_2) \mu e^{-2\lambda z_2} \left[\frac{df_1(z')}{dz'} \right] dz_2 dz'. \quad (\text{F12})$$

Using equation (E12) for the $\frac{df_1}{dz'}$ term in square brackets, this becomes

$$f_2' \Big|_{z=0} = -f_1(0) I(0, c) - \int_{z=0}^{\infty} \int_z^{\infty} \sigma(z_2) \mu e^{-2\lambda z_2} \left[e^{+2\lambda z'} \int_{z'}^{\infty} \sigma(z'') \mu e^{-2\lambda z''} dz'' \right] dz_2 dz', \quad (\text{F13})$$

where as usual, we have used $f_0 = 1$ in equation (E12) and we have used $I(\infty, c) = 0$ in the first term.

The integral over z'' can be recognized as $I(z', c)$, so this equation can be written

$$f_2' \Big|_{z=0} = -f_1(0)I(0, c) - \int_{z'=0}^{z'=\infty} \int_{z_2=z'}^{z_2=\infty} I(z', c) \sigma(z_2) e^{+2\lambda z'} \mu e^{-2\lambda z_2} dz_2 dz'. \quad (\text{F14})$$

Now, in equation (F14), make the substitution, $z_2 = z_3 + z'$, so $dz_2 = dz_3$ and the lower limit of the inner z_2 integration, which was $z_2 = z'$, becomes $z_3 = 0$. With the substitution, the positive exponential cancels and we have

$$f_2' \Big|_{z=0} = -f_1(0)I(0, c) - \int_{z'=0}^{z'=\infty} \int_{z_3=0}^{z_3=\infty} I(z', c) \sigma(z_3 + z') \mu e^{-2\lambda z_3} dz_3 dz'. \quad (\text{F15})$$

Rearranging and substituting the assumed form for the conductivity $\sigma(z_3 + z') = A_0 e^{-b(z_3 + z' - c)^2}$ and substituting $c_1 = c - z'$ gives

$$f_2' \Big|_{z=0} = -f_1(0)I(0, c) - \int_{z'=0}^{z'=\infty} \mu A_0 I(z', c) \int_0^{\infty} e^{-b(z_3 - c_1)^2} e^{-2\lambda z_3} dz_3 dz', \quad (\text{F16})$$

The remainder of the integrand after $I(z', c)$ in (F16) can be recognized from (F1) as $I(0, c_1) = I(0, c - z')$.

Therefore,

$$f_2' \Big|_{z=0} = -f_1(0)I(0, c) - \int_{z'=0}^{z'=\infty} I(z', c) I(0, c - z') dz'. \quad (\text{F17})$$

The integrals $I(z', c)$ and $I(0, c - z')$ can be evaluated using equation (F4). The z' integral must be evaluated numerically. When the upper limit was set to be too large, the error estimated by the quadrature algorithm was very large. We found that the best strategy for accurate results was to select a large upper limit (e.g. $z' = 500$ m or larger for resistive ground) and then, if the error estimated by the quadrature algorithm was too large, to halve this upper-limit iteratively until the desired accuracy was reached. This strategy was found to give results with a relative accuracy of 1 ppm.

The analytic expressions for f_1' can be simplified for the case of large b , but this has not been done in our implementation.

References

Abramowitz, M., and Stegun, I.A., 1972, Handbook of mathematical functions with formulas, graphs, and mathematical tables: National Bureau of Standards Applied Mathematics Series – 55.

Annan, A. P., Smith, R. S., Lemieux, J., O'Connell, M. D., and Pedersen, R. N., 1996, Resistive-limit time-domain AEM apparent conductivity: *Geophysics*, 61, 93-99. <https://doi.org/10.1190/1.1443960>

Bagley, T., and Smith, R. S. 2018, Estimating overburden thickness in resistive areas from two-component airborne EM data; *SEG International Exposition and 88th Annual Meeting*, 14-19 October 2018, Anaheim, CA, USA.

Bournas, N., Prikhodko, A., Kwan, K., Legault, J., Polianichko, V., and Treshchev, S., 2018, A new approach for kimberlite exploration using helicopter-borne TDEM data: *SEG Technical Program Expanded Abstracts 2018*, 1853-1857. doi: 10.1190/segam2018-2996206.1

Brand, L., 1960, *Advanced calculus: an introduction to classical analysis*, 3rd printing: Wiley.

Brown, J. W. and Churchill, R. V., 2004, *Complex variables and applications*, eighth edition: McGraw-Hill.

Desmarais, J. K., 2019a, On closed-form expressions for the approximate electromagnetic response of a sphere interacting with a thin-sheet — Part 1: Theory in the frequency and time domain: *Geophysics*, 84 (3), E199–E207. doi: 10.1190/geo2017-0498.1.

Desmarais, J. K., 2019b, On closed-form expressions for the approximate electromagnetic response of a sphere interacting with a thin sheet — Part 2: Theory in the moment domain, validation, and examples: *Geophysics*, 84 (3), E189–E198, doi: 10.1190/geo2019-0128.1

Fullagar, P. K., and Schaa, R., 2014, Fast 3D inversion of transient electromagnetic (TEM) resistive limit data: *SEG Technical Program Expanded Abstracts 2014*, 1827-1831.

<https://doi.org/10.1190/segam2014-1157.1>

Fullagar, P. K., Pears, G. A., Reid, J. E. and Schaa, R., 2015, Rapid approximate inversion of airborne TEM: *Exploration Geophysics*, **46**, 112-117. <https://doi.org/10.1071/EG14046>

Gel'fand, I. M., and Levitan, B. M., 1955: On the determination of a differential equation from its spectral function: *American Mathematical translations*, series 2, V 1, pp. 253-304.

Gray, M. C., 1933, Mutual impedance of long grounded wires when the conductivity of the earth varies exponentially with depth: *Physics*, 4, 75-80.

Guo, K., Mungall, J.E., and Smith, R.S., 2013, The ratio of B-field and dB/dt time constants from time-domain electromagnetic data: a new tool for estimating size and conductivity of mineral deposits, *Exploration Geophysics*, **44**, 238-244. doi: 10.1071/EG13042

Hall, D. 2014, Classification of cued metalmapper data using data mining techniques: *Symposium on the Application of Geophysics to Engineering and Environmental Problems 2014*, 443-451.

<https://doi.org/10.4133/SAGEEP.27-150>

Hyde, C., 2002, The electromagnetic response of a sphere in the moment domain: A building block for the construction of arbitrary 3D shapes: *SEG Technical Program Expanded Abstracts 2002*, 645-648.

<https://doi.org/10.1190/1.1817335>

Lee, T. J., and Iqnetik, R., 1994, Transient electromagnetic response of a halfspace with exponential conductivity profile and its applications to salinity mapping: *Exploration Geophysics*, 25, 39-51.

<https://doi.org/10.1071/EG994039>

Lee, T.J., Smith R.S., and Hyde, C.S.B., 2003a, A non-integer moment of the impulse response for a conductive halfspace: *Geophysical Prospecting*, **51**, 443-446.

<https://doi.org/10.1046/j.1365-2478.2003.00383.x>

Macnae, J.C., Smith, R.S., Polzer, B.D., Lamontagne, Y. and Klinkert, P.S., 1991, Conductivity-depth imaging of airborne electromagnetic step-response data: *Geophysics*, **56**, 102-114.

<https://doi.org/10.1190/1.1442945>

Morrison, H. F., Phillips, R. J. and O'Brien, D. P. 1969, Quantitative interpretation of transient electromagnetic fields over a layered half space: *Geophysical Prospecting*, **17**, 82 – 101. doi:

[10.1111/j.1365-2478.1969.tb02073.x](https://doi.org/10.1111/j.1365-2478.1969.tb02073.x)

Morse, P. M., and Feshbach, H., 1953: *Methods of theoretical physics, part II*, McGraw-Hill, Book Company, Inc. New York, Toronto, London.

Murray, S., 2017, Hankel documentation, release 0.3.5.

<https://media.readthedocs.org/pdf/hankel/stable/hankel.pdf>

Ogata, H., 2005, A numerical integration formula based on the Bessel functions, *Publications of the Research Institute for Mathematical Sciences*, 41 (4), 949-970. DOI: [10.2977/prims/1145474602](https://doi.org/10.2977/prims/1145474602)

Schaa, R., and Fullagar, P. K., 2010, Rapid, approximate 3D inversion of transient electromagnetic (TEM) data: *SEG Technical Program Expanded Abstracts 2010*, 650-654. <https://doi.org/10.1190/1.3513866>

Schaa, R. and Fullagar, P. K., 2012, Vertical and horizontal resistive limit formulas for a rectangular-loop source on a conductive half-space: *Geophysics*, **77 (1)**, E91-E99. <https://doi.org/10.1190/geo2011-0141.1>

Smith, R.S., 2000, The realizable resistive limit: A new concept for mapping geological features spanning a broad range of conductivities: *Geophysics*, **65**, 1124-1127. <https://doi.org/10.1190/1.1444805>

Smith, R.S., 2001, On removing the primary field from fixed-wing time-domain airborne electromagnetic data: some consequences for quantitative modelling, estimating bird position and detecting perfect conductors: *Geophysical Prospecting*, 49, 405-416. <https://doi.org/10.1046/j.1365-2478.2001.00266.x>

Smith, R., Fountain, D., and Allard, M., 2003b, The MEGATEM fixed-wing transient EM system applied to mineral exploration: a discovery case history: *First Break*, 21, July, 73-77.

Smith, R.S., and Lee, T.J., 2001, The impulse-response moments of a sphere in a uniform field, a versatile and efficient electromagnetic model: *Exploration Geophysics*, 32, 113-118.

<https://doi.org/10.1071/EG01113>

Smith, R.S., and Lee, T.J., 2002a, The moments of the impulse response: a new paradigm for the interpretation of electromagnetic data: *Geophysics*, 67, 1095-1103. <https://doi.org/10.1190/1.1500370>

Smith, R.S., and Lee, T.J., 2002b, Using the moments of a thick layer to map the conductance and conductivity from airborne electromagnetic data: *Journal of Applied Geophysics*, 49, 173-183.

[https://doi.org/10.1016/S0926-9851\(01\)00112-4](https://doi.org/10.1016/S0926-9851(01)00112-4)

Smith, R. S., and Lee, T. J., 2003, Errata To "The moments of the impulse response: A new paradigm for the interpretation of transient electromagnetic data" (Richard S. Smith and Terry J. Lee, *Geophysics*, 67, 1095–1103): *Geophysics*, 68 (1), 409 -409. <https://doi.org/10.1190/1.1553688>.

Smith, R.S. and Salem, A.S., 2007, A discrete conductor transformation of airborne electromagnetic data: *Near Surface Geophysics*, 5, 87-95. <https://doi.org/10.3997/1873-0604.2006021>

Smith, R.S., and Wasylechko, R., 2012, Sensitivity cross-sections in airborne electromagnetic methods using discrete conductors: *Exploration Geophysics*, 43, 95-103. <https://doi.org/10.1071/EG11048>

Smith, R.S., Hyde, C., Lee, T., Almond, R., 2003, Impulsive moments at work: *Proceedings of the 3DEM-3 symposium*, Australian Society of Exploration Geophysicists.

Smith, R.S., Lee, T.J., Annan, A.P., and O'Connell, M.D., 2005, Approximate apparent conductance (or conductivity) from the realizable moments of the impulse response: *Geophysics*, **70 (1)**, G29-G32.

<https://doi.org/10.1190/1.1852776>

Snyder, D. D., Prouty, M., George, D. C., King, T., Poulton, M., and Szidarovszky, A., 2010, UXO Discrimination at Camp San Luis Obispo with the Metalmapper: *Symposium on the Application of Geophysics to Engineering and Environmental Problems 2010*, 1054-1064. <https://doi.org/10.4133/1.3445421>

Titchmarsh, E. C., 1958: Eigenfunction expansions associated with second-order differential equations, Clarendon Press, Oxford

Watson, G. N. 1966, A treatise on the theory of Bessel functions, Cambridge University Press.

Weidelt, P., 1972: The inverse problem in geomagnetic induction, *Zeitschrift für Geophysik*, Band **38**, 257-289.